Journal of Applied Pharmaceutical Science Vol. 13(02), pp 089-098, February, 2023
Available online at http://www.japsonline.com
DOI: 10.7324/JAPS.2023.130210
ISSN 2231-3354

Profiling of α-glucosidase inhibitors from ethyl acetate fraction of Buas-buas (*Premna serratifolia*) leaves using UHPLC-Q-Orbitrap HRMS and protein–ligand interaction with molecular docking

Dini Hadiarti[1,2], Winarto Haryadi[1*], Sabirin Matsjeh[1], Respati Tri Swasono[1], Nurdianti Awaliyah[2]

[1]Department of Chemistry, Faculty of Mathematics and Natural Sciences, Universitas Gadjah Mada, Yogyakarta, Indonesia.
[2]Department of Chemistry Education, Muhammadiyah University of Pontianak, Indonesia.

ARTICLE INFO

Received on: 10/06/2022
Accepted on: 13/09/2022
Available Online: 05/02/2023

Key words:
Premna serratifolia, flavonoids, UHPLC-Q-Orbitrap HRMS, molecular docking, α-glucosidase, 2QMJ, 3TOP, 3A4A.

ABSTRACT

The Buas-buas (*Premna serratifolia*) leaves' extract from maceration, percolation, and decontamination have proven to be α-glucosidase inhibitors. Since the efforts to isolate phytochemical constituents from *P. serratifolia* leaves as α-glucosidase inhibitors have not been carried out, a study is needed to determine the responsible compound for this activity which has been proven *in vitro* and *in silico*. Isolation of active compounds from ethyl acetate fraction has the best inhibition utilizing column chromatography and semipreparative high-performance liquid chromatography (HPLC). Identifying compounds from the isolate was investigated by ultra-high-performance liquid chromatography-Q exactive hybrid quadrupole-orbitrap high-resolution mass spectrometry (UHPLC-Q-Orbitrap HRMS). Interaction of α-glucosidase and active compounds was studied by molecular docking utilizing N-terminal maltase-glucoamylase [protein data bank (PDB) code: 2QMJ], C-terminal maltase-glucoamylase (PDB code: 3TOP), and isomaltase (PDB code: 3A4A). Analyzed by UHPLC-Q-Orbitrap HRMS, nine flavonoids were detected, which are centaureidin, chrysin, pectolinaringenin, glycitein, kaempferide, syringetin, tricin, casticin, and 3,5,4′-trimethoxy-6,7-methylenedioxyflavone (estimated to be a new compound). Casticin–2QMJ, tricin–3TOP, and centaureidin–3A4A complexes have the lower binding energies of −5.29, −6.77, and −8.02 kcal/mol and inhibitory constant (Ki) of 131.54, 10.89, and 0.34 μM, sequentially.

INTRODUCTION

Premna serratifolia (*P. serratifolia*) L., a herbal medicinal plant locally known as Buas-buas, belongs to a diverse family of Lamiaceae. Traditionally, *P. serratifolia* leaves have been used as a tonic, treating headache, stomachache, diabetes, hypertension, difficulty in breathing, increasing breast milk production, and malaria (Dianita and Jantan, 2017; Hasanah *et al*., 2015). The scientific report showed that *P. serratifolia* leaves have been confirmed as hepatoprotection (Vadivu *et al*., 2009), antifungal (Wahyuni *et al*., 2014), antilarval (Lestari and Yanti, 2014), antioxidant (Isnindar *et al*., 2016), and α-glucosidase inhibitor (Hadiarti, 2017; Hadiarti *et al*., 2021; Simamora *et al*., 2020; Timotius *et al*., 2018).

Based on our previous study (Hadiarti *et al*., 2021), the phytochemical screening of ethyl acetate fraction of *P. serratifolia* leaves contained flavonoids, phenolics, and steroids. The metabolomic approach presented flavonoids which are the best contributor in inhibiting α-glucosidase. Although flavonoids have been known to greatly affect glucosidase inhibitory activity, the active compounds have not been identified.

Identified by liquid chromatography-mass spectrometry (LC-MS), caffeic acid in the decoction extract of *P. serratifolia* leaves is predicted to be an inhibitor of α-glucosidase (Timotius *et al*., 2018). The α-glucosidase inhibition activity from ethanol extract of *P. serratifolia* leaves was caused by scroside

*Corresponding Author
Winarto Haryadi, Department of Chemistry, Faculty of Mathematics and Natural Sciences, Yogyakarta, Indonesia.
E-mail: wnrt_haryadi @ ugm.ac.id

E, forsythoside A and forsythoside B, lavandulifolioside, diosmin, nobilin D, campneoside I, and isoacteoside, based on liquid chromatographyquadrupole time of flight-tandem mass spectrometry (LC-QTOF-MS/MS) analysis (Simamora *et al*., 2020). Efforts to isolate the active compound using either column chromatography or semipreparative HPLC have not been carried out by related researchers, so it is possible that the inhibitory activity could be caused by other compounds. In addition, UHPLC-Q-Orbitrap HRMS analysis, the most powerful analytical technique for detection and characterization in plant extract, has not been operated for profiling constituents that are primarily responsible for inhibiting α-glucosidase. Therefore, it is necessary to correctly identify α-glucosidase inhibitor compounds based on the metabolomic approach that we have done previously. Identification of α-glucosidase inhibitor compounds using UHPLC-Q-Orbitrap HRMS and molecular docking with N-terminal maltase-glucoamylase (2QMJ), C-terminal maltase-glucoamylase (3TOP), and isomaltase (3A4A) has been carried out in this research to prove the activity of these bioactive constituents *in silico*.

MATERIAL AND METHODS

Chemical

The organic solvents of analytical or HPLC grade, silica gel 60 (0.063–0.200 mm), and thin-layer chromatography (TLC) plate silica gel 60 F254 were obtained from Merck (Frankfurter Strasse, Darmstadt, Germany). All additional materials covering the α-glucosidase inhibition assay were produced from Sigma-Aldrich (St. Louis, USA).

Column chromatography of ethyl acetate extract of *P. serratifolia*

The extraction and fractionation procedures were carried out as reported by our research group (Hadiarti *et al*., 2021). The ethyl acetate fraction (16.24 g) is isolated by column chromatography (44 × 3.5 cm) utilizing eluent gradation from hexane, chloroform, and ethanol (100%:0%–0%:100%). According to TLC analysis, the same pattern of isolate was combined and obtained 24 fractions (F_1–F_{24}: 0.06, 0.05, 0.16, 0.14, 0.10, 0.12, 0.08, 0.12, 0.08, 0.06, 0.04, 0.04, 0.03, 0.03, 0.03, 0.03, 0.04, 0.034, 0.06, 0.02, 0.05, 0.05, 0.07, and 0.08 g, respectively).

α-glucosidase inhibition potential

The analysis of α-glucosidase inhibition was utilized by the chromogenic para-nitrophenyl-α-D-glucopyranoside (PNPG) method. Acarbose, an inhibitor of α-glucosidase, was reflected in the positive control, and para-nitrophenyl-α-D-glucopyranoside was used as substrate. The assay procedure was carried out in vitro of α-glucosidase inhibition reported by our research group.

Isolation by semipreparative HPLC

Three isolates (F_{12}–F_{14}: 0.04, 0.03, and 0.03 g, resp.) with better activity were separated by semipreparative HPLC (Waters 1525 Binary HPLC Pump). The isolation was operated using Waters Column Puresiel/Agilent Pursuit C18 (250 mm × 212 mm, 4 µl) and UV detector on λ 254 and 365 nm. The isolate (20 µl) was injected and flowed by 100 µl mobile phase [acetonitrile:water (0%:100%–100%:0%)] for 0–35 minutes on a flow rate of 1 ml/minute. Based on the chromatogram profile, the isolate was placed in a vial, evaporated, and resulted in 18 subfractions ($F_{12.1}$–$F_{12.6}$: 3.90, 4.36, 9.26, 2.34, 0.64, and 4.17 mg, $F_{13.1}$–$F_{13.6}$: 0.66, 4.38, 4.32, 1.67, 11.08, and 6.55 mg, and $F_{14.1}$–$F_{14.6}$: 1.16, 1.81, 2.75, 7.18, 4.43, and 7.79 mg, resp.).

UHPLC-UHPLC-Q-Orbitrap HRMS analysis

Identification of flavonoids from ethyl acetate subfraction of *P. serratifolia* was detected by UHPLC-Q-Orbitrap HRMS. The isolates were ultrasonically dissolved in 4 mL solvent (methanol:water) for 30 minutes at room temperature and filtrated by a polytetrafluoroethylene membrane filter with a pore size of 0.2 µm. The flavonoids were analyzed by Vanquish Flex UHPLC-Q Exactive Plus Orbitrap High-Resolution Mass Spectrometer applying AccucoreTM Phenyl Hexyl (100 × 2.1 mm, 2.6 µm) as the separation column and characterized by the arrangement of its scanning range from 50 to 1,500 m/z for tandem mass spectrometry (MS/MS) in the positive and negative mode of ionization. The mobile phase binary system was formulated by formic acid in water (A) and formic acid in acetonitrile (B) with gradient elution from 0–1 minute (5% B), 1–25 minutes (5%–95% B), 25–28 minutes (95% B), and 28–30 minutes (5% B). The flow rate was carried out at 0.25 ml/minute and an injection volume of 5 µl. Interpretation of data, including chosen spectra, aligned retention time (tR), and comparison with scientific database, was processed by Compound Discoverer version 2.2 (Farooq *et al*., 2020; Rafi *et al*., 2021; Umar *et al*., 2021).

In silico study

The studies of molecular docking were used to predict the binding modes of α-glucosidase protein and flavonoids using AutoDock Tools (version 1.5.6). The 3D flavonoid structures were downloaded from PubChem. The 2D 3,5,4′-trimethoxy-6,7-methylenedioxyflavone was drawn by ChemDraw Professional (version 17.1). All of the 3D flavonoid structures were converted to pdb. format using Open Bable GUI software (version 2.3). N-Terminal maltase-glucoamylase (2QMJ), C-terminal maltaseglucoamylase (3TOP), and isomaltase (3A4A) were obtained from Research Collaboratory for Structural Bioinformatics (RCSB) protein data bank (PDB). All flavonoids and protein were prepared for docking using Chimera (version 1.14). The grid box

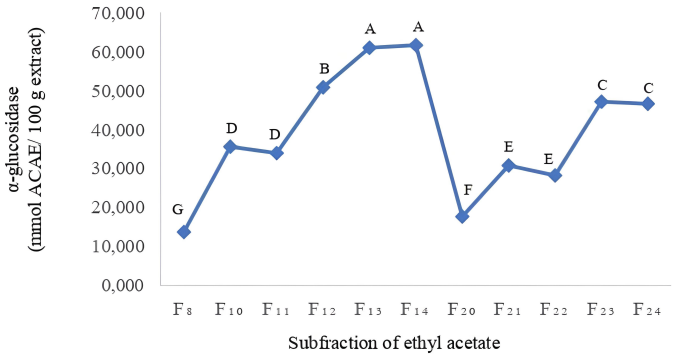

Figure 1. The α-glucosidase inhibition of ethyl acetate subfraction of leaves of *P. serratifolia*. Letters A–G indicate that the values are significant statistically at $p < 0.05$.

parameters were set at 40 × 40 × 40 Å to 2QMJ and 3A4A and 50 × 50 × 50 Å to 3TOP with a spacing of 0.375 Å centered on macromolecules. The molecular docking was operated by the Lamarckian genetic algorithm with 100 runs, 150 populations, and 2,500,000 energy evaluations. The interaction of flavonoids and protein was visualized using Biovia Discovery Studio Visualizer (version 2021) (Cai *et al*., 2020; Zhang *et al*., 2017).

Statistical analysis

The data evolution of difference from the subfraction ethyl acetate of the α-glucosidase inhibitory activity was investigated by analysis of variance (ANOVA) with Tukey's test ($p < 0.05$) applying XLSAT 5.03 software Addinsoft (New York, America).

RESULT AND DISCUSSION

α-Glucosidase inhibitor activity

Based on our previous research (Hadiarti *et al*., 2021), the ethyl acetate fraction of *P. serratifolia* is the best α-glucosidase inhibitor (77.63 ± 0.18 mg Acarbose equivalent (ACAE)/100 g extract) From Figure 1, among 24 subfractions of ethyl acetate, F_{12}–F_{14} are found to be highly potent inhibitors of α-glucosidase (50.915, 61.041, and 61.746 mmol ACAE/ 100 g extract, respectively). Compared to α-glucosidase inhibition activity of control, F_{12}–F_{14} subfractions of ethyl acetate are 0.53, 0,63, and 0.64 times than acarbose. Compared to infusion and decoction extracts (4.27 and 0.046 µg Gallic acid equivalent (GAE)/mL) (Timotius *et al*., 2018), the α-glucosidase inhibition of F_{12}–F_{14} subfractions is weak because of the use of different positive control, namely gallic acid.

Profile of flavonoids

The identification of α-glucosidase inhibitor from a fractioned subfraction of ethyl acetate by UHPLC-Q-Orbitrap HRMS is presented in Table 1 and Figure 2. The interpretation of spectra MS^1 and MS^2 is focused on flavonoids which have the highest correlation with acarbose equivalent (Hadiarti *et al*., 2021). There are nine flavonoids divided into three groups which are flavone (centaureidin, chrysin, 3,5,4′-trimethoxy-6,7-methylenedioxyflavone, syringetin, pectolinaringenin, tricin, and casticin), isoflavone (glycitein), and flavanol (kaempferide). There is no reference containing spectra and ion pattern of 3,5,4′-trimethoxy-6,7-methylenedioxyflavone, so it is predicted as a new compound. In previous studies on the genus Premna, only kaempferide has been identified from *P. schimperi* (Dianita and Jantan, 2017). The results of this study are different from previous studies that have identified the presence of phenolic compounds, flavonoid derivate, and bibenzyl derivative that are predicted to be α-glucosidase inhibitors from *P. serratifolia* (Simamora *et al*., 2020; Timotius *et al*., 2018).

Table 1. UHPLC-Q-Orbitrap HRMS flavonoids profile of F_{12}–F_{14} subfractions of ethyl acetate fraction of *P. serratifolia*.

Subfraction	Compound	Retention time (minute)	Molecular formula	Theory mass (*m/z*)	Experiment mass (*m/z*)	Accuracy (ppm)	Ion MS^2 (m/z)	Reference
$F_{12.4}$	Centaureidin	14.54	$C_{18}H_{16}O_8$	360.08452	360.08306	−4.05	346.06784; 209.63461	PubChem
$F_{12.5}$	Chrysin	11.15	$C_{15}H_{10}O_4$	254.05791	254.05653	−5.43	209.05879; 153.01813	(Wang *et al*., 2020; Zhao *et al*., 2018)
$F_{14.6}$		15.12						
$F_{12.5}$	Glycitein	15.27	$C_{16}H_{12}O_5$	284.06847	284.06674	−6.11	270.05167; 242.05692	(Andres *et al*., 2015)
$F_{12.6}$		8.35						
$F_{13.6}$		15.31						
$F_{14.6}$		15.27						
$F_{12.6}$	3,5,4′-Trimethoxy-6,7-methylenedioxyflavone	13.90	$C_{19}H_{16}O_7$	356.08960	356.08853	−3.02	339.08603; 311.09122; 297.07544	-
$F_{12.6}$	Kaempferide	15.63	$C_{16}H_{12}O_6$	300.06339	300.06240	−3.30	151.03915; 107.04931	PubChem
$F_{12.6}$	Pectolinarigenin	16.10	$C_{17}H_{14}O_6$	314.07904	314.07966	1.97	298.04794; 298.04794; 283.02451	(Gong *et al*., 2016; Velamuri *et al*., 2020)
$F_{13.4}$	Syringetin	12.34	$C_{17}H_{14}O_8$	346,06887	346.06707	−5.20	301.06970; 151.03864	(Baron *et al*., 2020; Wang *et al*., 2020)
$F_{13.5}$		12.29						
$F_{14.5}$	Tricin	12.71	$C_{17}H_{14}O_7$	330.07395	330.07257	−4.20	316.05722; 98.98434	(Zengin *et al*., 2019)
$F_{13.6}$	Casticin	15.01	$C_{19}H_{18}O_8$	374.10017	374.09890	−3.39	360.08289; 342.07266	(Han *et al*., 2007; Lewin et al., 2010; Mahomoodally *et al*., 2019; Nadeem *et al*., 2020)
$F_{14.6}$		14.99						

Accuracy for Q-Orbitrap analyzer < 5 ppm (Arrebola-Liébanas *et al*., 2017).

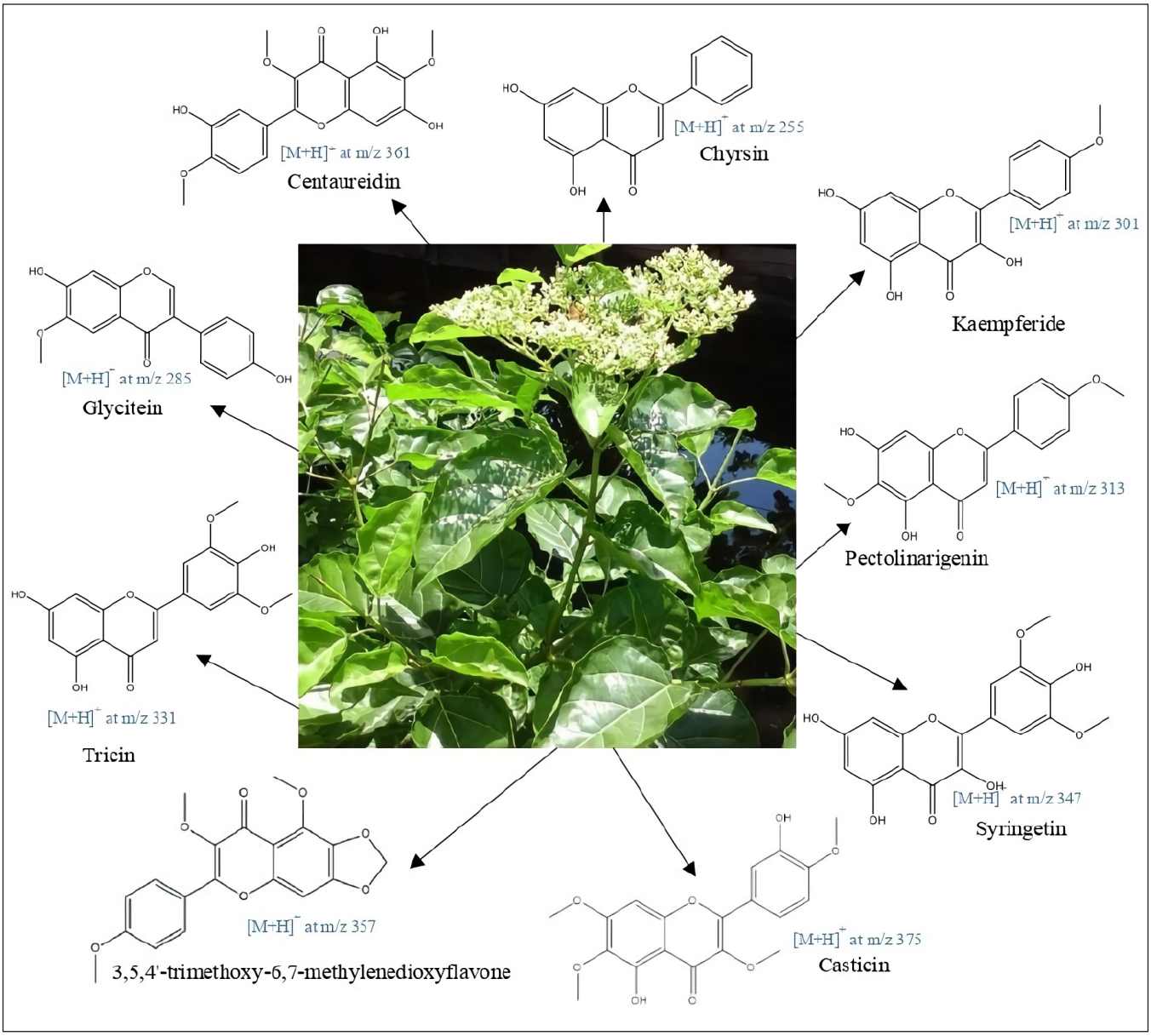

Figure 2. Proposed structures of identified flavonoids from ethyl acetate subfraction leaves' extract of *P. serratifolia*.

According to Table 2, seven of nine flavonoids have been approved as α-glucosidase inhibitors, while 3,5,4′-trimethoxy-6,7-methylenedioxyflavone and casticin have not been investigated. Syringetin exhibited the highest α-glucosidase inhibitor. Compared to other flavones, syringetin has more hydroxyl groups than centaureidin, chrysin, tricin, and pectolinaringenin, so that is predicted as the reason for the lowest IC_{50}.

Molecular docking

The interaction study of flavonoids within the active site of 2QMJ, 3TOP, and 3A4A was clarified by molecular docking analysis. The binding energy, inhibition constant (Ki), hydrogen bond, and hydrophobic interaction are parameters for selecting the best performance of flavonoids to inhibit α-glucosidase. The low binding energy indicates high bond stability so that the potential for flavonoid interaction with protein will increase. The inhibition constant is an indicator of flavonoid concentration for inhibiting α-glucosidase enzyme performance. The more the hydrogen bond occurs, the more stable the structure of flavonoids and proteins is formed. The hydrophobic interactions, which are aliphatic–aromatic, aromatic–aliphatic, aliphatic–aliphatic, carbon–halogen, and sulfur–aromatic, increase the high efficiency of flavonoids as a ligand (Freitas and Schapira, 2017; Holdgate *et al*., 2018; Ramsay and Tipton, 2017).

The results of molecular docking in Table 3. displayed those complexes of 2QMJ with glycitein, 3,5,4′-trimethoxy-6,7-methylenedioxyflavone, kaempferide, pectolinaringenin, tricin, and casticin has lower binding energy than acarbose-2QMJ. Centaureidin, chrysin, glycitein, 3,5,4′-trimethoxy-6,7-methylenedioxyflavone, pectolinaringenin, syringetin, and casticin

Table 2. IC_{50} of α-glucosidase inhibition from nine flavonoids.

Flavonoids	IC_{50} (μM)	Reference
Centaureidin	>250	(Thien *et al*., 2017)
Chrysin	422.67	(Li *et al*., 2018)
Glycitein	150	(Zhang *et al*., 2016)
Kaempferide	646.70	(Quan *et al*., 2020)
Pectolinarigenin	230	(Amin *et al*., 2017)
Syringetin	36.80	(Wu *et al*., 2016)
Tricin	91.50	(Nguyen *et al*., 2017)
Acarbose	996.02	(Li *et al*., 2018)

Table 3. Binding energy of Ki, H-bond, and hydrophobic interaction.

Compound	Protein	$\Delta G_{binding}$ (kcal/mol)	Ki (μM)	H-bond	Hydrophobic interaction
Acarbose (native ligan)	2QMJ	−3.59	2,350	TYR605, ASP327, HIS600, ARG526, ASP542, and ASP203	-
	3TOP	−4.67	375.02	ASP1526, ASP1157, ASP1279, HIS1584, and ARG1510	TRP1355, YR1251, and PHE1559
	3A4A	−1.50	79,700	LYS406, ASN401, and GLU405	-
Quersetin (control ligan)	2QMJ	−4.74	334.32	ASP542, ARG202, THR205, and ASN207	LEU473 and THR204
	3TOP	−5.81	55.67	ASP1157, ASP1279, and HIS1584	TRP1355
	3A4A	−6.41	19.68	ASP233, ASN317, GLU422, and GLY161	PHE314 and ALA418
Centaureidin	2QMJ	−3.48	2,790	ASP542, THR205, and GLN603	GLN603, PHE575, and TYR605
	3TOP	−6.48	17.71	LYS1460, ASP1157, TRP1369, HIS1584, and ASP1526	TRP1369,T YR1251, PHE1560, ILE1315, and TRP1418
	3A4A	−8.02	0.34	LYS373, ASN564, GLU562, and LYS568	PRO567, LYS568, and PHE494
Chyrsin	2QMJ	−3.55	2,510	ARG526 and ASP542	TRP406, TYR299, TRP406
	3TOP	−5.87	49.99	ASP1279, HIS1584, ASP1420, and ARG1510	PHE1560, TYR1251, TRP1355, PHE1560, and TYR1251
	3A4A	−7.65	2.47	LYS373, ASN489, and ASN493	PHE494 and LYS568
Glycitein	2QMJ	−3.8	1,630	ASP203 and GLN603	MET444, PHE450, TYR299, ALA576, TYR605, and PHE575
	3TOP	−6.32	23.47	ASP1279, ARG1510, and ASP1157	PHE1559, HIS1584, TRP1418, TRP1253, TYR1251, PHE1559, and TRP1335
	3A4A	−7.80	1.90	PRO488	PHE494, LYS568
3,5,4′-Trimethoxy-6,7-methylenedioxyflavone	2QMJ	−4.63	402.11	ASN209, ARG202, and THR205	THR204, LYS480, and LEU473
	3TOP	−6.47	18.11	HIS1584 and LYS1460	TYR1521, PHE1559 PHE1427, TRP1369, LYS1460, PHE1559, TRP1523, TRP1418
	3A4A	−3.81	1,620	-	VAL319, PRO320, LYS432, and LEU318

Continued

Compound	Protein	$\Delta G_{binding}$ (kcal/mol)	Ki (μM)	H-bond	Hydrophobic interaction
Keampfride	2QMJ	−3.77	1,730	ASP474	PRO198
	3TOP	−5.19	156.29	ASP1279, HIS1584, ASP1470, and ARG1510	TRP1355 PHE1559, TYR1251, and TRP1369
	3A4A	−3.19	4,580	LYS324, GLU322, and ASP521	ILE328 and LYS324
Pectolinarigenin	2QMJ	−4.07	1,050	ASN209, ARG202, THR205, ASP203, and ASP542	THR204, LEU473, and THR406
	3TOP	−5.73	62.75	ASP1420, HIS1584, ASP1279, ARG1510, and LYS1460	MET1421, PHE1559, and TRP1335 ILE1315, TRP1418, HIS1584, LYS1460, and TRP1369
	3A4A	−7.84	1.80	ASN415 and GLU422	HIS423, PHE314, TRP238, ALA418, ILE419, and LYS432
Syringetin	2QMJ	−3.54	2,540	GLN603, ARG334, and ASP203	TRP406, PHE450, and TYR299
	3TOP	−6.71	12.04	ASP1157, ASP1279, and HIS1584	TRP1355, TYR1251, MET1421, RP1355, ILE1315, ILE1280, HIS1584, PHE1559, TRP1523, and TRP1418
	3A4A	−7.84	1.80	GLU497, GLU562, LYS568, GLY564, LYS373, and ASN489	PHE568, PHE493, and PRO567
Tricin	2QMJ	−4.01	1,140	ASP203 and GLN603	TRP406, TYR299, TYR605, PHE575, and ALA576
	3TOP	−6.77	10.89	ASP1157, THR1586, HIS1584, and ASP1279	TRP1355, TYR1251, PHE1559, TRP1418, TRP1523, HIS1584, ILE1315, and ILE1280
	3A4A	−7.12	6.06	LYS568, LYS373, ASN489, and ASN493	PHE494, LEU561, and VAL571
Casticin	2QMJ	−5.29	131.54	ARG202, ASN207, THR205, ASP542, and TYR214	LEU473 and THR204
	3TOP	−6.37	21.45	HIS1584, ASP1279, ARG1520, ASP1157, and LYS1480	PHE1559, HIS1584, TRP1418, ILE1315, TRP1523, PHE1559, and PRO1159
	3A4A	−8.00	1.36	ASN259, HIS295, LYS16, THR290, and ASP341	ALA292, TRP15, LYS13, and ILE262

complex with 3TOP have comparably presented better binding energy than acarbose-3TOP. This result is in accordance with the preceding study, which informed that the identified compounds have better binding energy than acarbose (Murugesu *et al*., 2018, 2019; Nokhala *et al*., 2020). There is no native ligand for 3A4A in PDB, but molecular docking with acarbose was performed and resulted in inferior binding energy than identified flavonoids.

According to Table 3., quercetin, as a control ligand, formed a complex of 2QMJ and resulted in the weakest binding energy compared to nine flavonoids, except casticin. Meanwhile, the quercetin–3TOP complex showed the lowest binding energy except for kaempferide and pectolinaringenin. Quercetin–3A4A complex had higher binding energy than cantharidin, chrysin, glycitein, pectolinaringenin, syringetin, tricin, and casticin. The results are similar to a previous report; flavonoids and protein complexes, such as baicalein–2QMJ, cathecin–2QMJ, and cathecin–3TOP, have better binding energy than quercetin (Zhang *et al*., 2017).

Among the identified flavonoids of *P. serratifolia* with the α-glucosidase inhibition activity, flavone complex with 2QMJ, 3TOP, or 3A4A has the best binding energy, followed by isoflavone and flavanol. The binding energy of the flavone–2QMJ complex increases in the following order: casticin <3,5,4′-trimethoxy-6,7-methylenedioxyflavone < pectolinaringenin < tricin < chrysin < syringetin < centaureidin. The interactions between 3TOP and flavones in the following order from the lowest to the highest binding energy were tricin < syringetin < centaureidin < 3,5,4′-trimethoxy-6,7-methylenedioxyflavone < casticin < chrysin

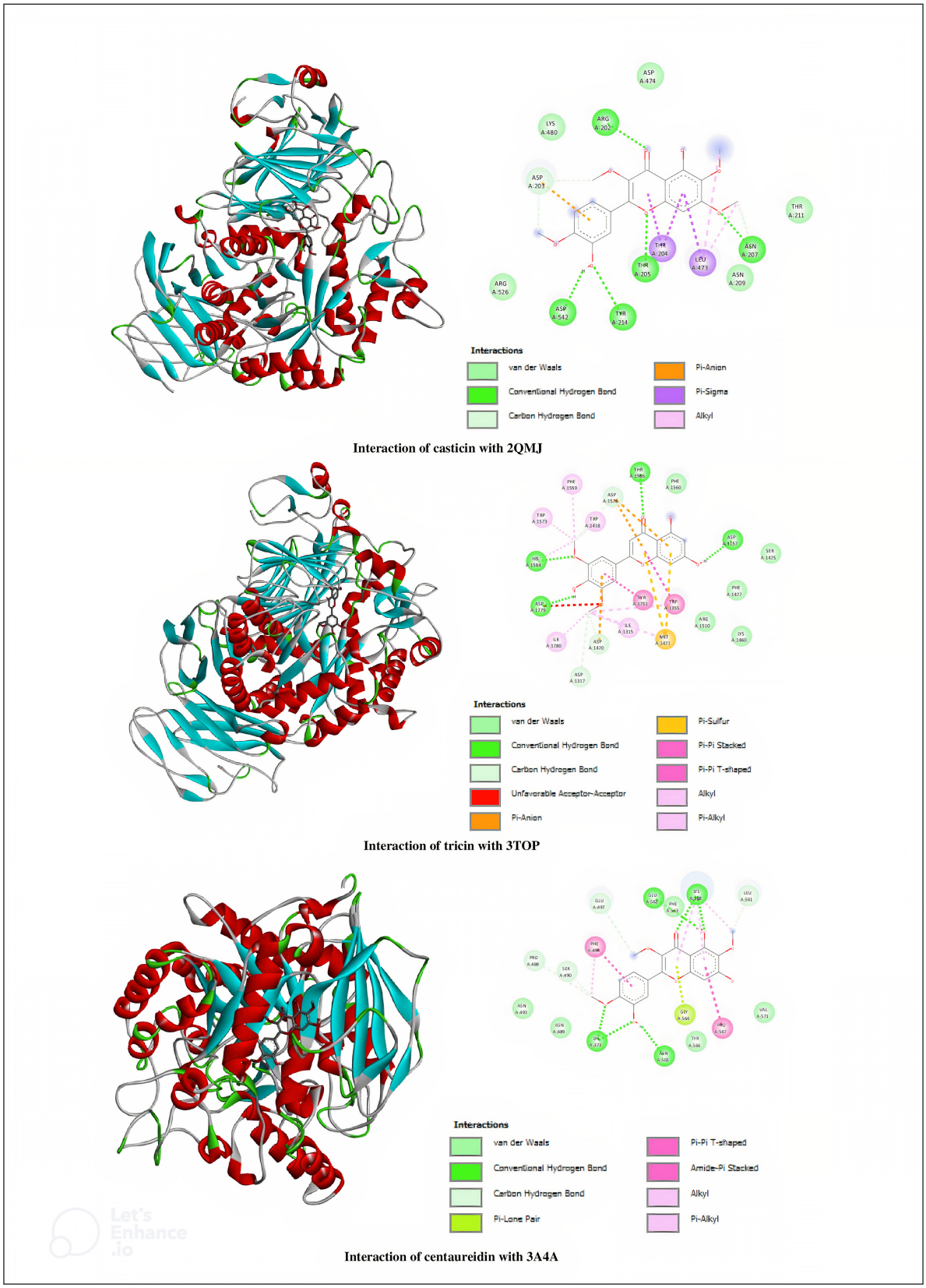

Figure 3. 3D and 2D diagrams presenting the interaction of casticin, tricin, and centaureidin as potential inhibitors with 2QMJ, 3TOP, and 3A4A.

< pectolinaringenin. The binding energy of centaureidin is smaller than casticin < pectolinaringenin < syringetin < chrysin < tricin < 3,5,4′-trimethoxy-6,7-methylenedioxyflavone when formed complex of 3A4A.

The crystal structure of the N-terminal subunit of the human maltase-glucoamylase (2QMJ) is mainly arranged of monomeric subunit, chain-A with a sequence length of 870 amino acids. Casticin has performed the best binding energy and inhibition constant with 2QMJ toward the other flavonoids. From *in silico* study, casticin is stabilized by five hydrogen bonds between ASN207 and methoxy group in the A-ring, ARG202 and THR205 and carbonyl and ether groups, and ASP542 and TYR214 and the hydroxyl group in the C-ring. The total number of hydrophobics was observed in three interactions which are π-sigma between LEU473 and THR204 in the A- and C-rings and π-alkyl between LEU473 and methyl group in the A-ring. Based on binding energy, Ki, and the similarity of hydrogen interactions that occur in quercetin and 2QMJ (ASP542, ARG202, THR205, and ASN207 residues), casticin has more potential as an α-glucosidase inhibitor compared to other flavonoids, native, and control ligand.

The C-terminal subunit of the human maltase-glucoamylase enzyme is composed of two chains, A and B, with a sequence length of 908 amino acids. Compared to the other flavonoids, tricin is the lowest binding energy and inhibition constant docked with 3TOP. Four residues, including ASP1157, THR1586, HIS1584, and ASP1279, were investigated to interact hydrogen interactions between hydroxyl groups in A-, C-, and B-rings. Formed hydrophobic interactions, tricin interacted with TRP1355 and A-ring by π-π stacked, TYR1251 and π-π T-shaped, and PHE1559, TRP1418, TRP1523, HIS1584, ILE1315, ILE1280, MET1421, and TRP1355 with B-ring by alkyl/π-alkyl. Tricin which has three residues (ASP1157, HIS1584, and ASP1279) the same as hydrogen-bonded quercetin–3TOP has the finest α-glucosidase inhibitory action compared to the other flavonoids, native ligand, and control ligand since it has the least binding energy and Ki.

Isomaltase crystal structure with PDB: 3A4A is arranged by a chain-A sequence length of 589 amino acids. Centaureidin–3A4A complex showed the lowest binding energy and inhibition constant among nine flavonoids. A total of six hydrogen bonds were formed between LYS568 and GLU562 to the hydroxyl group in the A-ring, LYS568 to the carbonyl group in the C-ring, and LYS373 and ASN564 to the hydroxyl group and LYS373 to methoxy group in the B-ring. Residue PRO567 interacted with the A-ring by hydrophobic π-π T-shaped, and methyl group in the A- and B-ring formed π-alkyl interaction with LYS568 and PHE494. The interaction between centauredin and 3A4A has the lowest binding energy and Ki compared to acarbose, quercetin, and the other flavonoids, so it is more potential as an α-glucosidase inhibitor.

The results of the molecular docking study were in accordance with the in vitro α-glucosidase inhibition test, which showed that the F_{14} fraction had the best activity. The identification by UHPLC-Q-Orbitrap HRMS showed chrysin, glycitein, tricin, and casticin contained in the F_{14} fraction. The casticin–2QMJ and tricin–3TOP complexes obtain the lowest binding energy differentiated from other flavonoids, native ligand, and control ligand. Meanwhile, the smallest binding energy of the flavonoid complex with 3A4A occurred in centaureidin, which was −8.02 kcal/mol. However, this binding energy value is 0.2 less than the casticin–3A4A complex, which reaches −8.00 kcal/mol.

CONCLUSION

$F_{14,}$ which contains chrysin, glycitein, tricin, and casticin, is the fraction with the best α-glucosidase inhibition. According to references and molecular docking studies, flavones (centaureidin, chrysin, tricin, 3,5,4′-trimethoxy-6,7-methylenedioxyflavone, pectolinaringenin, syringetin, and casticin) that are semipolar have better α-glucosidase inhibitory activity than isoflavones (glycitein) and flavanols (kaempferide). Nine flavonoids except kaempferide were first reported from the genus *Premna,* and 3,5,4’-trimethoxy-6,7-methylenedioxyflavone was predicted as a new compound. Casticin, tricin, and centaureidin in a single compound were flavones which will be antidiabetic potential as α-glucosidase inhibitor examined *in vitro*, *in silico*, and *in vivo*.

AUTHOR CONTRIBUTIONS

All authors made substantial contributions to conception and design, acquisition of data, or analysis and interpretation of data; took part in drafting the article or revising it critically for important intellectual content; agreed to submit to the current journal; gave final approval of the version to be published; and agree to be accountable for all aspects of the work. All the authors are eligible to be an author as per the international committee of medical journal editors (ICMJE) requirements/guidelines.

FUNDING

There is no funding to report.

CONFLICTS OF INTEREST

The authors report no financial or any other conflicts of interest in this work.

ETHICAL APPROVALS

This study does not involve experiments on animals or human subjects.

DATA AVAILABILITY

All data generated and analyzed are included within this research article.

PUBLISHER’S NOTE

This journal remains neutral with regard to jurisdictional claims in published institutional affiliation.

REFERENCES

Amin A, Tuenter E, Foubert K, Iqbal J, Cos P, Maes L, Exarchou V, Apers S, Pieters L. *In Vitro* and *In Silico* Antidiabetic and Antimicrobial Evaluation of Constituents from *Kickxia ramosissima* (*Nanorrhinum ramosissimum*). Front Pharmacol, 2017; 8(232):1–12.

Andres S, Hansen U, Niemann B, Palavinskas R, Lampen A. Determination of the isoflavone composition and estrogenic activity of commercial dietary supplements based on soy or red clover. Food Funct, 2015; 6(6):2017–25.

Arrebola-Liébanas FJ, Romero-González R, Garrido-Frenich A. HRMS: Fundamentals and Basic Concepts. In: Applications in High Resolution Mass Spectrometry: Food Safety and Pesticide Residue Analysis. In: Romero-González,R. and Frenich,A.G. (eds). Elsevier Inc, Amsterdam, pp. 1-14, 2017

Baron G, Altomare A, Regazzoni L, Fumagalli L, Artasensi A, Borghi E, Ottaviano E, Del Bo C, Riso P, Allegrini P, Petrangolini G, Morazzoni P, Riva A, Arnoldi L, Carini M, Aldini G. Profiling *Vaccinium macrocarpon* components and metabolites in human urine and the urine ex-vivo effect on *Candida albicans* adhesion and biofilm-formation. Biochem Pharmacol, 2020; 173(113726):1–15.

Cai Y, Wu L, Lin X, Hu X, Wang L. Phenolic profiles and screening of potential α-glucosidase inhibitors from *Polygonum aviculare* L. leaves using ultra-filtration combined with HPLC-ESI-QTOF-MS/MS and molecular docking analysis. Indus Crops Prod, 2020; 154(112673):1–11.

Dianita R, Jantan I. Ethnomedicinal uses, phytochemistry and pharmacological aspects of the genus premna: a review. Pharm Biol, 2017; 55(1):1715–39.

Farooq MU, Mumtaz MW, Mukhtar H, Rashid U, Akhtar MT, Raza SA, Nadeem M. UHPLC-QTOF-MS/MS based phytochemical characterization and anti-hyperglycemic prospective of hydro-ethanolic leaf extract of *Butea monosperma*. Sci Rep, 2020; 10(1):1–15.

Freitas RFD, Schapira M. A systematic analysis of atomic protein-ligand interactions in the PDB †. MedChemComm, 2017; 8(10):1970–81.

Gong J, Miao H, Sun XM, Hou WE, Chen JH, Xie ZY, Liao Q.F. Simultaneous qualitative and quantitative determination of phenylethanoid glycosides and flavanoid compounds in: *Callicarpa kwangtungensis* Chun by HPLC-ESI-IT-TOF-MS/MS coupled with HPLC-DAD. Anal Methods, 2016; 8(33):6323–36.

Hadiarti D. *In vitro* α-glucosidase inhibitory activity of ethanol extract of Buas-buas (*Premna serratifolia* Linn). Tradit Med J, 2017; 22(2):80–83.

Hadiarti D, Haryadi W, Matsjeh S, Swasono RT. Understanding phytochemical roles on α-glucosidase inhibitory activity based on metabolomic approach of *Premna serratifolia* leaves from West Borneo, Indonesia. Rasayan J Chem, 2021; 14(02):1216–22.

Han X, Ma X, Zhang T, Zhang Y, Liu Q,Ito Y. Isolation of high-purity casticin from *Artemisia annua* L. by high-speed counter-current chromatography. J Chromatogr A, 2007; 1151(1–2):180–2.

Hasanah S, Wibowo MA, Idiawati N. Toksisitas *Lygodium microphyllum*, *Premna serratifolia* L. dan *Vitex pinnata* asal Desa Kuala Mandor B. Jurnal Kimia Khatulistiwa, 2015; 4(4):101–5.

Holdgate GA, Meek TD, Grimley RL. Mechanistic enzymology in drug discovery: a fresh perspective. Nat Rev Drug Discov, 2018; 17(2):115–32.

Isnindar, Subagus W, Widyarini S, Yuswanto. Determenation of antioxidant activities of Buas-buas (*Premna serratifolia* L.) using DPPH (2,2-diphenyl-1- picrylhydrazyl) method. Tradit Med J, 2016; 21(3):111–5.

Lestari MA, Yanti AH. Uji Aktivitas Ekstrak Metanol dan n-Heksan Daun Buas-Buas (*Premna serratifolia* Linn.) Pada Larva Nyamuk Demam Berdarah (*Aedes aegypti* Linn.). Protobiont, 2014; 3(2):247–51.

Lewin G, MacIuk A, Thoret S, Aubert G, Dubois J, Cresteil T. Semisynthesis of natural flavones inhibiting tubulin polymerization, from Hesperidin. J Nat Prod, 2020; 73(4):702–6.

Li K, Yao F, Xue Q, Fan H, Yang L, Li X, Sun L, Liu Y. Inhibitory effects against α-glucosidase and α-amylase of the flavonoids-rich extract from *Scutellaria baicalensis* shoots and interpretation of structure–activity relationship of its eight flavonoids by a refined assign-score method. Chem Central J, 2018; 12(1):1–11.

Mahomoodally MF, Zengin G, Aladag MO, Ozparlak H, Diuzheva A, Jekő J, Cziáky Z, Aumeeruddy MZ. HPLC-MS/MS chemical characterization and biological properties of *origanum onites* extracts: a recent insight. Int J Environ Health Res, 2019; 29(6):607–21.

Murugesu S, Ibrahim Z, Ahmed QU, Uzir BF, Nik-Yusoff NI, Perumal V, Abas F, Shaari K, Khatib A. Identification of α-glucosidase inhibitors from *Clinacanthus nutans* leaf extract using liquid chromatography-mass spectrometry-based metabolomics and protein-ligand interaction with molecular docking. J Pharm Anal, 2019; 9(2):91–9.

Murugesu, S., Ibrahim, Z., Ahmed, Q. U., Yusoff, N. I. N., Uzir, B. F., Perumal, V., Abas, F., Saari, K., El-Seedi, H., & Khatib, A. Characterization of α-glucosidase inhibitors from *Clinacanthus nutans* Lindau leaves by gas chromatography-mass spectrometry-based metabolomics and molecular docking simulation. Molecules, 2018; 23(9):1–21.

Nguyen TT, Nguyen DH, Zhao BT, Le DD, Choi DH, Kim YH, Nguyen TH, Woo MH. A New lignan and a new alkaloid, and α-glucosidase inhibitory compounds from the grains of *Echinochloa utilis* Ohwi & Yabuno. Bioorgan Chem, 2017; 74:221–7.

Nokhala A, Siddiqui MJ, Ahmed QU, Bustamam MSA, Zakaria ZA. Investigation of α-glucosidase inhibitory metabolites from *Tetracera scandens* leaves by GC–MS metabolite profiling and docking studies. Biomolecules, 2020; 10(2):1–17.

Quan YS, Zhang XY, Yin XM, Wang SH, Jin LL. Potential α-glucosidase inhibitor from *Hylotelephium erythrostictum*. Bioorgan Med Chem Lett, 2020; 30(24):127665.

Rafi M, Septaningsih DA, Karomah AH, Lukman, Prajogo B, Amran MB, Rohman A. Inhibition of α-glucosidase activity, metals content, and phytochemical profiling of *Andrographis Paniculata* from different geographical origins based on FTIR and UHPLC-Q-Orbitrap HRMS metabolomics. Biodiversitas, 2021; 22(3):1535–42.

Ramsay RR, Tipton KF. Assessment of enzyme inhibition: a review with examples from the development of monoamine oxidase and cholinesterase inhibitory drugs. Molecules, 2017; 22(1192):1–47.

Simamora A, Santoso AW, Timotius KH, Rahayu I. Antioxidant activity, enzyme inhibition potentials, and phytochemical profiling of *Premna serratifolia* L. leaf extracts. Int J Food Sci, 2020; 2020:1–11.

Tan L, Jin Z, Ge Y, Nadeem H, Cheng Z, Azeem F, Zhan R. Comprehensive ESI-Q TRAP-MS/MS based characterization of metabolome of two mango (*Mangifera indica* L) Cultivars from China. Sci Rep, 2020; 10(1):1–19.

Thien T, Huynh V, Vo L, Tran N, Luong T, Le T, Duc T, That Q. Two new compounds and α-glucosidase inhibitors from the leaves of *Bidens pilosa* L. Phytochemistry Letters, 2017; 20(2017):119–22.

Timotius KH, Simamora A, Santoso AW. Chemical characteristics and *in vitro* antidiabetic and antioxidant activities of *Premna serratifolia* L. leaf infusion and decoction. Pharmacogn J, 2018; 10(6):1114–8.

Umar AH, Ratnadewi D, Rafi M, Sulistyaningsih YC. Untargeted metabolomics analysis using FTIR and UHPLC-Q-Orbitrap HRMS of two Curculigo species and evaluation of their antioxidant and α-glucosidase inhibitory activities. Metabolites, 2021; 11(1):1–17.

Vadivu R, Suresh AJ, Girinath K, Kannan PB, Vimala R, Kumar NMS. Evaluation of hepatoprotective and *in-vitro* cytotoxic activity of leaves of *Premna serratifolia* Linn. J Sci Res, 2009; 1(1):145–52.

Velamuri R, Sharma Y, Fagan, J, Schaefer J. Application of UHPLC-ESI-QTOF-MS in phytochemical profiling of Sage (*Salvia officinalis*) and Rosemary (R*osmarinus officinalis*). Planta Med Int Open, 2020; 07(04):e133–44.

Wahyuni S, Mukarlina, Yanti AH. Aktivitas Antifungi Ekstrak Metanol Daun Buas-Buas (*Premna serratifolia*) Terhadap Jamur Diplodia sp. Pada Jeruk Siam (*Citrus nobilis* var . microcarpa). Protobiont, 2014; 3(2):274–9.

Wang L, Tan N, Wang H, Hu J, Diwu W, Wang X. A systematic analysis of natural α-glucosidase inhibitors from flavonoids of *Radix scutellariae* using ultrafiltration UPLC- TripleTOF-MS/MS and network pharmacology. BMC Complement Med Ther, 2020; 20(71):1–17.

Wu B, Song HP, Zhou X, Liu XG, Gao W, Dong X, Li HJ, Li P, Yang H. Screening of minor bioactive compounds from herbal medicines by *in silico* docking and the trace peak exposure methods. J Chromatogr A, 2016; 1436:91–9.

Zengin G, Aumeeruddy MZ, Diuzheva A, Jekő J, Cziáky Z, Yıldıztugay A, Yıldıztugay E, Mahomoodally MF. A Comprehensive appraisal on *Crocus chrysanthus* (Herb.) herb. flower extracts with HPLC-MS/MS profiles, antioxidant and enzyme inhibitory properties. J Pharm Biomed Anal, 2019; 164:581–9.

Zhang BW, Li X, Sun WL, Xing Y, Xiu ZL, Zhuang CL, Dong YS. Dietary flavonoids and acarbose synergistically inhibit α-glucosidase and lower postprandial blood glucose. J Agric Food Chem, 2017; 65(38):8319–30.

Zhang Y, Wang N, Wang W, Wang J, Zhu Z, Li X. Molecular mechanisms of novel peptides from Silkworm Pupae that inhibit α-glucosidase. Peptides, 2016; 76(2016):45–50.

Zhao X, Su X, Liu C, Jia Y. Simultaneous determination of chrysin and tectochrysin from *Alpinia oxyphylla* Fruits by UPLC-MS/MS and its application to a comparative pharmacokinetic study in normal and dementia rats. Molecules, 2018; 23(7):1–11.

How to cite this article:
Hadiarti D, Haryadi W, Matsjeh S, Swasono RT, Awaliyah N. Profiling of α-glucosidase inhibitors from ethyl acetate fraction of Buas-buas (*Premna serratifolia*) leaves using UHPLC-Q-orbitrap HRMS and protein–ligand interaction with molecular docking. J Appl Pharm Sci, 2023; 13(02): 089–098.